

Banner appropriate to article type will appear here in typeset article

Buoyancy effects on film boiling heat transfer from a sphere at low velocities.

Rishabh Singh, Anikesh Pal[†], and Santanu De

Department of Mechanical Engineering, Indian Institute of Technology Kanpur, INDIA

(Received xx; revised xx; accepted xx)

A theoretical model is developed for the forced convection film boiling phenomenon over a heated sphere moving vertically downwards in the water. Unprecedented to the previous analytical studies, this model accounts for the buoyancy effects while solving the momentum, and energy equations in the vapor phase to obtain the velocity, and the temperature distribution in terms of the vapor boundary layer thickness. To calculate the vapor boundary layer thickness an energy balance is applied at the vapor-liquid interface. The flow of liquid around the sphere is considered to be governed by the potential theory, and the energy equation in liquid is then solved for the known velocity distribution. We find that the vapor boundary layer thickness increases with an increase in the sphere, and the bulk water temperature, and a decrease in the free stream velocity. This further results in a decrease in the film boiling heat transfer coefficient. The present study concludes that at low free stream velocities (< 0.5 m/s) buoyancy becomes significant in delaying the separation, and when the velocity is further reduced the separation angle approaches 180° .

Key words:

1. Introduction

The knowledge of heat-transfer rates from spherical particles at high flux levels can significantly contribute towards designing energy systems associated with space industries and nuclear reactors. The primary mode of heat transfer in such energy systems is film boiling in which a vapor layer wraps the heated spherical surface preventing its contact with the liquid. Film boiling can be characterized as natural convection film boiling and forced convection film boiling. In natural convection film boiling the motion of the liquid over the heated specimen is caused by the viscous drag forces of the rising vapor acting on the liquid whereas in forced convection film boiling the liquid is forced to flow over the heated specimen. The information about the film boiling phenomenon can be used to determine core cooling-ability after certain hypothetical nuclear accidents that result in extensive core melting. The concept of film boiling has also been utilized in the area of naval applications for drag reduction techniques by inserting a vapor layer in between the surface, and the

[†] Email address for correspondence: pala@iitk.ac.in

surrounding liquid (Vakarelski *et al.* 2011).

Theoretical and experimental investigation on film boiling of saturated liquid such as carbon tetrachloride, benzene, ethyl alcohol, n-hexane over a cylinder were performed by Bromley *et al.* (1953). They reported that for high velocity flows the separation angle was close to 90° , whereas for sufficiently low velocities the separation angle approaches 180° . Motte & Bromley (1957) used the same experimental setup as Bromley *et al.* (1953) with some modifications to study subcooled (when the temperature of the liquid is below its boiling point) forced convection film boiling over a cylinder with turbulence. It was found that with an increase in subcooling and velocity, the heat transfer rate also increases. Bradfield (1967) also studied film boiling over a sphere using experimental techniques, and concluded that minimum superheat required to sustain the film boiling increases linearly with an increase in subcooling. Transient subcooled forced convection film boiling over a sphere was experimentally investigated by Walford (1969). Different regimes of film boiling over the sphere have been identified, and the subsequent heat flux behavior in those regimes was reported.

Kobayasi & Kiyosi (1965) theoretically investigated film boiling heat transfer from a sphere moving downward in a liquid and proposed a general solution for predicting the boiling heat transfer coefficient as a function of certain parameters such as Reynolds number, liquid-vapor viscosity ratio, Prandtl number, size of the sphere, the kinematic viscosity of the liquid. However, the findings of Kobayasi & Kiyosi (1965) were not accurate owing to the incorrect pressure used for the theoretical derivation (Hesson & Witte 1966).

To derive the theoretical heat transfer rate Bromley *et al.* (1953); Kobayasi & Kiyosi (1965) used imposed pressure gradient from the free stream. Additionally, Bernoulli's theorem was applied to get an additional equation in terms of the frictional loss in vapor. The problem was further simplified by considering saturated liquid flow around the body. When the liquid is at saturation temperature there will be no heat flux going into the bulk liquid, and all the heat leaving the sphere is used in vaporizing and superheating the vapor. As the heat transfer phenomenon is straightforward in the case of saturated liquid, the energy conservation equation is not solved, and the calculations in the liquid become simple. However, in practical situations, the liquids are not saturated. Therefore, an energy equation should be solved both in the liquid and the vapor phase to obtain an accurate temperature distribution to properly characterize the heat transfer process around the body. In the present investigation, we solve the energy equation in both the liquid and the vapor phases to obtain the temperature distribution in both phases.

Witte (1967, 1968*a,b*); Witte & Orozco (1984) carried out experimental and theoretical investigations of forced convection film boiling from a sphere moving in a liquid. The experiment of Witte (1968*a*) used a transient technique in which a heated sphere attached to a swinging-arm apparatus was passed through a pool of liquid sodium. The heat transfer rates from the sphere to liquid sodium were measured, and were found to be in good agreement with the theoretical expressions for heat transfer from a sphere during forced convection with the assumption of potential flow in liquid sodium. Witte (1968*b*) assumed a linear profile for velocity in the vapor film and reported the forced convection film boiling from a sphere in a saturated liquid. The effect of non-linear velocity profile within the vapor film on subcooled flow film boiling from a sphere is analyzed by Witte (1967); Witte & Orozco (1984). While calculating the vapor boundary layer thickness Witte (1967) neglected the effect of radiation, and argued that for highly subcooled liquid the energy required for the

vaporization of liquid can be ignored in comparison to the heat energy going into the bulk liquid. In contrast, Witte & Orozco (1984) included the heat energy required to vaporize the liquid and concluded that the results based on the non-linear velocity profile produce results comparable to the experiments. The liquid velocity at the vapor-liquid interface was calculated from the potential flow theory in all the investigations. Additionally these theoretical investigations did not consider buoyancy in their analysis. We will demonstrate in section 3 that buoyancy plays a crucial role in obtaining results that are similar to the experiments.

Dhir & Purohit (1978) performed theoretical and experimental investigation to determine the effect of flow velocity, subcooling, initial sphere temperature on film boiling heat transfer from a sphere. Their theoretical analysis although included the effect of buoyancy was restricted only to natural convection film boiling over a sphere where the surrounding liquid was stagnant. The vapor film was assumed to be stable, and very thin in comparison to the radius of the sphere so that the non-linear behavior of the film can be neglected. With an increase in both sphere, and bulk water temperature Dhir & Purohit (1978) observed a decrease in the film boiling heat transfer coefficient owing to an increase in the vapor film thickness. They also reported that the minimum temperature to sustain a stable film depends only on subcooling, and increases linearly with subcooling.

An experimental study of transient film boiling on different geometries (spheres, cylinders, flat plates) with different coolant velocities was also conducted by Jauhara & P.Axcell (2009). Their study on the nature of the vapor/liquid interface and the collapse modes has revealed a new model for film collapse, in which an explosive liquid-solid contact is followed by film re-formation and the motion of a quench front over the hot surface. The heat transfer coefficients, and heat fluxes during film boiling were found essentially to depend on the temperature of the body, and water subcooling. A theoretical model was also developed that predicted the heat transfer coefficients to within 10% of experimental values for water subcooling above 10K. However, their theoretical model was restricted to plane surfaces only.

In this investigation, we develop a theoretical model to determine the heat transfer characteristics and boundary layer separation behavior owing to film boiling from a heated spherical particle moving slowly in water under the influence of buoyancy unprecedented to the earlier theoretical studies. A comparison of our theoretical model with the experimental study of Jauhara & P.Axcell (2009), and the theoretical model of Witte & Orozco (1984) is also performed to assess the efficacy of our model.

The methodology for the development of the theoretical model is presented in section 2. Results from our model are discussed in section 3 and the conclusions drawn from this study are given in section 4.

2. Methodology

The schematic of film boiling over a sphere is shown in figure 1. When the liquid comes in contact with the heated sphere, a vapor layer is formed around the sphere as the temperature of the sphere is higher than the saturation temperature of the liquid. Heat conduction occurs through the vapor layer. A portion of this heat is utilized in vaporizing the liquid that adds to the vapor layer, increasing the vapor layer thickness. Another portion of the heat is diffused into the bulk liquid. Figure 1 manifests the vapor layer and the liquid layer around the sphere.

The vapor boundary layer moves past the heated sphere and is influenced by both the sphere and the liquid layer. The liquid layer only feels the influence of the vapor layer and is not in direct contact with the sphere. We aim to theoretically determine the heat transfer rates during the film boiling from the sphere including the effects of buoyancy. Our analysis is based on the following assumptions:

- (i) liquid-vapor interface is smooth and is in dynamic equilibrium,
- (ii) the temperature of the sphere is uniform,
- (iii) physical properties of vapor and liquid are evaluated at mean film temperature,
- (iv) heat transfer across the vapor layer take place by conduction only,
- (v) inertial effects in the momentum and energy equations are neglected,
- (vi) the flow of liquid around the sphere is governed by potential flow theory,
- (vii) vapor film is axially symmetric.

All of the above-mentioned assumptions are justified from the available theoretical and experimental studies. Bradfield (1966) observed that the ripples formed during film boiling in the surrounding liquid at rest tends to dampen as the liquid starts moving. As the velocity of the liquid around the body is increased the liquid-vapor interface becomes unstable. The velocity range we use in the current investigation is smaller than that can cause an unstable interface and therefore, it is reasonable to assume a smooth liquid-vapor interface. The uniformity of the temperature of the sphere is justified for low Biot numbers. Bradfield (1967) also found that the maximum discrepancy in heat flux calculations was less than 2% if uniform temperature distribution is assumed within the specimen as compared to the case when calculations are performed considering variability in temperature distribution within the sphere. The physical properties of the vapor and the liquid phase were computed by Bromley *et al.* (1953) from well-defined expressions developed to calculate the average value of the physical property. However, it was concluded that for simplicity all physical properties can be evaluated at the mean film temperature except for the latent heat of vaporization. This justifies our third assumption. Burns (1989) concluded that the film thickness obtained experimentally, and calculated assuming heat transfer across the film by conduction manifest no significant difference. Therefore, the heat transfer across the vapor film can be assumed to take place solely by conduction. Similar assumptions were made by Bromley *et al.* (1953); Motte & Bromley (1957). Our fifth assumption is justified owing to the fact that the thickness of the vapor layer is very small in comparison to the diameter of the sphere (Bromley *et al.* 1953; Witte 1967; Kobayasi & Kiyosi 1965; Witte & Orozco 1984; Jouhara & P.Axcell 2009). Assumption 6 is justified from the study of Kutateladze (1959) where it has been shown that the assumption of potential flow or viscous flow in the liquid does not make a significant difference.

2.1. *Liquid region*

According to the sixth assumption, the velocity distribution in bulk liquid is:

$$u_r = -3U \frac{r-R}{R} \cos \theta \quad , \quad u_\theta = \frac{3}{2}U \sin \theta, \quad (2.1)$$

where, θ is the azimuthal angle measured from the stagnation point, r is the radial direction, U is the incoming free stream velocity of liquid, u_r is the velocity in the radial direction, u_θ is the velocity in the azimuthal direction, R is the radius of the sphere.

From figure 1, we can write:

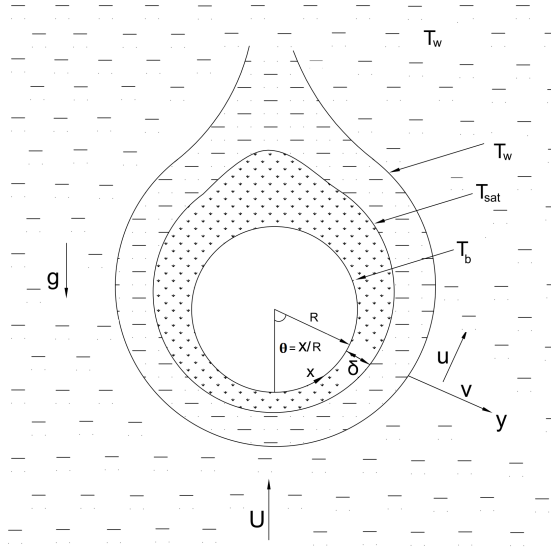


Figure 1: Schematic of film boiling over a sphere.

- (i) $y = r - R$,
- (ii) $\theta = \frac{x}{R}$,

where x is the curvilinear coordinate along the surface of the sphere, and y is the curvilinear coordinate normal to the x direction.

We can transform u_r and u_θ in curvilinear coordinate system as follows:

$$u_r = -3U \frac{r-R}{R} \cos \theta = -3U \frac{y}{R} \cos \frac{x}{R}, \quad (2.2)$$

$$u_\theta = \frac{3}{2}U \sin \theta = \frac{3}{2}U \sin \frac{x}{R}, \quad (2.3)$$

Next, we consider the energy equation for the liquid in the spherical coordinates system:

$$u_r \frac{\partial T}{\partial r} + \frac{u_\theta}{r} \frac{\partial T}{\partial \theta} + \frac{u_\phi}{r \sin \theta} \frac{\partial T}{\partial \phi} = \alpha_l \left(\frac{\partial^2 T}{\partial r^2} + \frac{2}{r} \frac{\partial T}{\partial r} \right). \quad (2.4)$$

where α_l is the thermal diffusivity of liquid and T is temperature. Since the flow is assumed to be axially symmetric and there is no component of velocity in the ϕ direction, we can write equation 2.4 as follows:

$$u_r \frac{\partial T}{\partial r} + \frac{u_\theta}{r} \frac{\partial T}{\partial \theta} = \alpha_l \left(\frac{\partial^2 T}{\partial r^2} + \frac{2}{r} \frac{\partial T}{\partial r} \right). \quad (2.5)$$

Sideman (1966) demonstrated that if heat transfer is assumed to take place in a thin layer near the interface, the term scaling with $\frac{1}{r} \frac{\partial T}{\partial r}$ can be neglected in comparison to the term $\frac{\partial^2 T}{\partial r^2}$. Therefore, under this assumption we can modify the equation 2.5 as follows:

$$u_r \frac{\partial T}{\partial r} + \frac{u_\theta}{r} \frac{\partial T}{\partial \theta} = \alpha_l \frac{\partial^2 T}{\partial r^2}. \quad (2.6)$$

We use the information from figure 1 for the following transformations:

$$u_\theta = u_l, u_r = v_l; x = r\theta \implies dx = r d\theta; y = r - R \implies dy = dr, \quad (2.7)$$

where, u_l and v_l are the velocities of the liquid in x and y directions respectively. Substituting 2.7 in equation 2.6 we get,

$$u_l \frac{\partial T}{\partial x} + v_l \frac{\partial T}{\partial y} = \alpha_l \frac{\partial^2 T}{\partial y^2} \quad (2.8)$$

The boundary conditions corresponding to equation 2.8 considering $R + \delta \sim R$ are as follows:

- (i) $y \rightarrow \infty, T = T_w, \theta \geq 0,$
- (ii) $y = 0, T = T_{sat}, \theta \geq 0,$
- (iii) $0 < y \leq \infty, T = T_w, \theta = 0.$

Here, T_{sat} is the saturation temperature of the liquid, T_w is the temperature of bulk water, δ is the vapor layer thickness. We transform equation 2.8 using the following variables such that the solution of the transformed equations is known.

$$\Delta T = T - T_{sat}, \psi = y \sin^2 \theta, \eta = \int_0^\theta \sin^3 \theta d\theta = -\frac{3}{4} \cos \theta + \frac{1}{12} \cos 3\theta + \frac{2}{3}. \quad (2.9)$$

Now, consider the following derivatives

$$\frac{\partial T}{\partial y} = \frac{\partial \Delta T}{\partial y} = \frac{\partial \Delta T}{\partial \psi} \frac{\partial \psi}{\partial y} + \frac{\partial \Delta T}{\partial \eta} \frac{\partial \eta}{\partial y} = \frac{\partial \Delta T}{\partial \psi} \sin^2 \theta. \quad (2.10)$$

$$\frac{\partial^2 T}{\partial y^2} = \frac{\partial^2 \Delta T}{\partial y^2} = \frac{\partial}{\partial y} \left(\frac{\partial \Delta T}{\partial y} \right) = \frac{\partial}{\partial \psi} \left(\frac{\partial \Delta T}{\partial \psi} \sin^2 \theta \right) \frac{\partial \psi}{\partial y} + \frac{\partial}{\partial \eta} \left(\frac{\partial \Delta T}{\partial \psi} \sin^2 \theta \right) \frac{\partial \eta}{\partial y} = \sin^4 \theta \frac{\partial^2 \Delta T}{\partial \psi^2}. \quad (2.11)$$

$$\frac{\partial T}{\partial x} = \frac{\partial \Delta T}{\partial x} = \frac{\partial \Delta T}{\partial \psi} \frac{\partial \psi}{\partial x} + \frac{\partial \Delta T}{\partial \eta} \frac{\partial \eta}{\partial x} = 2 \frac{y}{R} \sin \theta \cos \theta \frac{\partial \Delta T}{\partial \psi} + \left(\frac{3}{4R} \sin \theta - \frac{1}{4R} \sin 3\theta \right) \frac{\partial \Delta T}{\partial \eta}. \quad (2.12)$$

Substituting equations 2.2, 2.3, 2.10, 2.11, 2.12 in equation 2.8, we get:

$$\frac{\partial \Delta T}{\partial \eta} = \frac{2R\alpha_l}{3U} \frac{\partial^2 \Delta T}{\partial \psi^2}. \quad (2.13)$$

Using $M = \frac{2R\alpha_l}{3U}$, we can write:

$$\frac{\partial \Delta T}{\partial \eta} = M \frac{\partial^2 \Delta T}{\partial \psi^2}. \quad (2.14)$$

The boundary conditions corresponding to equation 2.14 are:

- (i) $\psi \rightarrow \infty, \eta \geq 0, \Delta T = T_w - T_{sat}$,
- (ii) $\psi = 0, \eta \geq 0, \Delta T = 0$,
- (iii) $0 < \psi \leq \infty, \eta = 0, \Delta T = T_w - T_{sat}$.

Solution of equation 2.14 subjected to the above boundary conditions can be found by defining $\beta = \frac{T - T_w}{T_{sat} - T_w}$ and using it in equation 2.14 to get:

$$\frac{\partial \beta}{\partial \eta} = M \frac{\partial^2 \beta}{\partial \psi^2}. \quad (2.15)$$

The boundary conditions corresponding to equation 2.15 are:

- (i) $\psi \rightarrow \infty, \eta \geq 0, \beta = 0$,
- (ii) $\psi = 0, \eta \geq 0, \beta = 1$,
- (iii) $0 < \psi \leq \infty, \eta = 0, \beta = 0$.

The partial differential equation 2.15 can be converted to ordinary differential equation using method of combination of variable. Defining $\beta = \psi^a \eta^b$, where a and b are constants and substituting in equation 2.15 we get:

$$\frac{\psi^2}{M\eta} = \frac{a(a-1)}{b} = \text{Constant} \quad (2.16)$$

The new variable can be of the form $\left(\frac{c\psi^2}{M\eta}\right)^d$. Let us define the new variable as $\gamma = \frac{\psi}{\sqrt{4M\eta}}$ (obtained by choosing $d = 1/2$ and $c = 1/4$) and hence we can write $\beta(\psi, \eta) = \beta(\gamma)$.

$$\frac{\partial \beta}{\partial \eta} = \frac{d\beta}{d\gamma} \frac{\partial \gamma}{\partial \eta} = -\frac{\psi}{2\eta\sqrt{4\eta M}} \frac{d\beta}{d\gamma} \quad (2.17)$$

$$\frac{\partial^2 \beta}{\partial \psi^2} = \frac{1}{4M\eta} \frac{d^2 \beta}{d\gamma^2} \quad (2.18)$$

Substituting equation 2.17 and 2.18 in equation 2.15, we get an ordinary differential equation as follows:

$$\frac{d^2 \beta}{d\gamma^2} + 2\gamma \frac{d\beta}{d\gamma} = 0. \quad (2.19)$$

The boundary conditions corresponding to equation 2.19 will become:

- (i) $\gamma = 0, \beta = 1$,
- (ii) $\gamma = \infty, \beta = 0$.

The solution of equation 2.19 is of the form:

$$\beta = B + A \int_0^\gamma e^{-\gamma^2} d\gamma, \quad (2.20)$$

and applying the boundary conditions will result in:

$$\frac{T - T_w}{T_{sat} - T_w} = \operatorname{erfc} \left(\frac{\psi}{2\sqrt{M\eta}} \right) \quad (2.21)$$

Equation 2.21 represents the temperature distribution in the liquid, and we can use it to calculate the heat flux, q_b'' , into the bulk liquid as follows:

$$q_b'' = -k_l \left(\frac{\partial T}{\partial y} \right) \Big|_{y=0}, \quad (2.22)$$

where k_l is the thermal conductivity of the liquid.

Using equations 2.10 and 2.21 we get,

$$\frac{\partial T}{\partial y} \Big|_{y=0} = - \frac{(T_{sat} - T_w) \sin^2 \theta}{\sqrt{\pi M \eta}}, \quad (2.23)$$

$$q_b'' = \frac{k_l \Delta T_w \sin^2 \theta}{\sqrt{\pi M \eta}}. \quad (2.24)$$

2.2. Vapor region

We write the momentum equation in the x direction in the vapor region following figure 1 as follows:

$$\rho_v \left(u \frac{\partial u}{\partial x} + v \frac{\partial u}{\partial y} \right) = - \frac{\partial p}{\partial x} + \Delta \rho g \sin \theta + \mu_v \frac{\partial^2 u}{\partial y^2}, \quad (2.25)$$

where $\Delta \rho = \rho_l - \rho_v$, ρ_l and ρ_v are the densities of liquid and vapor respectively and g is the acceleration due to gravity, u and v are the velocities of the vapor in x and y directions respectively. Application of the fifth assumption results in the following equation:

$$\frac{\partial^2 u}{\partial y^2} = \frac{1}{\mu_v} \left(\frac{\partial p}{\partial x} - \Delta \rho g \sin \theta \right). \quad (2.26)$$

The boundary conditions corresponding to equation 2.26 are,

- (i) $y = 0$, $u = 0$,
- (ii) $y = \delta$, $u = \frac{3}{2} U \sin \theta$.

Since the vapor layer thickness (δ) is thin, the streamwise variation of pressure in the liquid layer as given by the Bernoulli equation is impressed on the vapor layer (Witte 1967). Therefore, using Bernoulli's equation in the liquid layer we can write:

$$p + \frac{1}{2} \rho_l u_l^2 = \text{Constant}. \quad (2.27)$$

Here u_l is the velocity in the liquid. Differentiating equation 2.27 with respect to x we obtain:

$$\frac{\partial p}{\partial x} = -\rho_l u_l \frac{du_l}{dx}. \quad (2.28)$$

From equations 2.2 and 2.7 we can write $u_l = \frac{3}{2} U \sin \theta = \frac{3}{2} U \sin \frac{x}{R}$ and modify equation

2.28 as follows:

$$\frac{dp}{dx} = -\rho_l u_l \frac{du_l}{dx} = -\frac{9}{8} \left(\frac{\rho_l U^2}{R} \right) \sin 2\theta. \quad (2.29)$$

Substituting equation 2.29 in equation 2.26 and solving for the corresponding boundary conditions we get,

$$u = \frac{3}{2} U \sin \theta \frac{y}{\delta} + \left(\frac{9}{8} \frac{\rho_l U^2}{\mu_v R} \sin \theta \cos \theta + \frac{\Delta \rho g \sin \theta}{2\mu_v} \right) (y\delta - y^2) \quad (2.30)$$

We can see that the velocity in equation 2.30 is comprised of a linear term, $\frac{3}{2} U \sin \theta \frac{y}{\delta}$, and two non-linear terms, $\frac{9}{8} \frac{\rho_l U^2}{\mu_v R} \sin \theta \cos \theta$, and $\frac{\Delta \rho g \sin \theta}{2\mu_v}$. The first non-linear is due to the imposed pressure gradient by the potential flow of liquid, whereas the second non-linear term represents the effect of buoyancy. Witte & Orozco (1984) in their theoretical model did not consider buoyancy effects. Therefore, if we neglect the buoyancy, then non-linearity in the velocity profile is sustained only by the imposed pressure. We can further see that the first non-linear term is proportional to the square of the velocity, and at low velocities, the non linear term is dominated by the buoyancy effects.

2.3. Temperature distribution in Vapor layer

In equation 2.30 the vapor layer thickness, δ , is an unknown. Determination of δ is important for understanding the heat transfer phenomenon. To compute δ we start with the energy equation for the vapor layer in the x direction as follows:

$$u \frac{\partial T}{\partial x} + v \frac{\partial T}{\partial y} = \alpha \frac{\partial^2 T}{\partial y^2}. \quad (2.31)$$

The corresponding boundary conditions for 2.31 are:

- (i) $y = 0$, $u = 0$, $T = T_b$,
- (ii) $y = \delta$, $u = \frac{3}{2} U \sin \theta$, $T = T_{sat}$,

where T_b is the temperature of the sphere. Using assumptions 4 and 5, equation 2.31 can be written, and solved as follows:

$$\frac{\partial^2 T}{\partial y^2} = 0 \implies T = C_1 y + C_2. \quad (2.32)$$

Substituting the corresponding boundary condition in equation 2.32 we get,

$$T = T_b + (T_{sat} - T_b) \frac{y}{\delta}. \quad (2.33)$$

This equation represents the temperature distribution in the vapor layer.

2.4. Vapor boundary layer thickness

Next, we consider the heating provided by the sphere that results in the vaporization of liquid at the vapor-liquid interface, and superheating of the newly formed vapor above T_{sat} . Also, since the bulk water is below the saturation temperature, a part of total heat energy available at the vapor-liquid interface due to conduction across the vapor film, and radiation from the sphere goes into the bulk liquid. From the energy balance on a differential element as shown

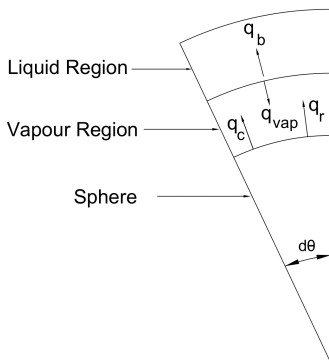


Figure 2: Energy balance over elemental area of sphere.

in figure 2 we can write,

$$dq_c + dq_r = dq_{vap} + dq_b, \quad (2.34)$$

where,

- (i) dq_c is heat transfer due to conduction across vapor film, $q_c'' = \frac{k_v(T_b - T_{sat})}{\delta}$ (we get by substituting equation 2.33 in the Fourier's law of heat conduction,
- (ii) dq_r is heat transfer due to radiation , $q_r'' = \sigma \epsilon (T_b^4 - T_{sat}^4)$
- (iii) dq_{vap} is heat utilised in vaporizing the liquid.
- (iv) dq_b is sensible heat energy going in water, $q_b'' = \frac{k_l \Delta T_w \sin^2 \theta}{\sqrt{\pi M \eta}}$

The energy flux utilised in vaporization of liquid can be written as,

$$dq_{vap} = h'_{fg} dw = h'_{fg} d(\rho_v A_c \bar{u}), \quad (2.35)$$

where dw is the increase of mass flow rate in vapor layer due to vaporization, h_{fg} is the latent of vaporization, $h'_{fg} = h_{fg} \left(1 + \frac{0.4 C_{pl}(T_b - T_{sat})}{h_{fg}} \right)$ is the modified latent heat of vaporization (Bromley *et al.* 1953; Witte 1967; Witte & Orozco 1984) that accounts for the temperature variation in the vapor field and super heating of vapor above T_{sat} , $A_c = 2\pi R \delta \sin \theta$ is the flow cross section of the film, and \bar{u} is the average vapor velocity at any θ .

The average velocity in the vapor film is calculated as follows:

$$\bar{u} = \frac{1}{\delta} \int_0^{\delta} u dy = \frac{1}{\delta} \int_0^{\delta} \left(\frac{3}{2} U \sin \theta \frac{y}{\delta} + \left(\frac{9}{8} \frac{\rho_l U^2}{\mu_v R} \sin \theta \cos \theta + \frac{\Delta \rho g \sin \theta}{2 \mu_v} \right) (y \delta - y^2) \right) dy \quad (2.36)$$

\Rightarrow

$$\bar{u} = \frac{3}{4} U \sin \theta + \frac{3 \rho_l U^2}{16 \mu_v R} \sin \theta \cos \theta \delta^2 + \frac{\Delta \rho g \sin \theta}{12 \mu_v} \delta^2 \quad (2.37)$$

Using equation 2.37 in equation 2.35,

$$dq_{vap} = h'_{fg} d \left(\rho_v 2\pi R \delta \sin \theta \left(\frac{3}{4} U \sin \theta + \frac{3 \rho_l U^2}{16 \mu_v R} \sin \theta \cos \theta \delta^2 + \frac{\Delta \rho_l g \sin \theta}{12 \mu_v} \delta^2 \right) \right) \quad (2.38)$$

⇒

$$dq_{vap} = h'_{fg} \frac{d}{d\theta} \left(\rho_v 2\pi R \delta \sin\theta \left(\frac{3}{4} U \sin\theta + \frac{3\rho_l U^2}{16\mu_v R} \sin\theta \cos\theta \delta^2 + \frac{\Delta\rho_l g \sin\theta}{12\mu_v} \delta^2 \right) \right) d\theta \quad (2.39)$$

From equation 2.34 we can write,

$$\frac{k_v (T_b - T_{sat})}{\delta} dA + q''_r dA = dq_{vap} + q''_b dA, \quad (2.40)$$

⇒

$$dq_{vap} = \frac{k_v (T_b - T_{sat})}{\delta} dA + q''_r dA - q''_b dA$$

, ⇒

$$\frac{dq_{vap}}{dA} = \frac{k_v (T_b - T_{sat})}{\delta} + q''_r - q''_b$$

where, $dA = 2\pi R^2 \sin\theta d\theta$ is the differential area element on the sphere, and k_v is the thermal conductivity of the vapor. Substituting, dA , q''_r and q''_b in above equation, we get

$$\frac{dq_{vap}}{2\pi R^2 \sin\theta d\theta} = \frac{k_v (T_b - T_{sat})}{\delta} + \sigma \epsilon (T_b^4 - T_{sat}^4) - \frac{k_l \Delta T_w \sin^2 \theta}{\sqrt{\pi M \eta}}, \quad (2.41)$$

Substituting equation 2.39 in 2.41, and separating $\frac{d\delta}{d\theta}$ we obtain:

$$\frac{d\delta}{d\theta} = \frac{\frac{k_v (T_b - T_{sat})}{\delta} + \sigma \epsilon (T_b^4 - T_{sat}^4) - \frac{k_l \Delta T_w \sin^2 \theta}{\sqrt{\pi M \eta}} - \frac{h'_{fg} \rho_v}{R} \left(\frac{3U \cos\theta \delta}{2} + \frac{3\rho_l U^2}{16\mu_v R} (3 \cos^2 \theta - 1) \delta^3 + \frac{\Delta\rho_l g \cos\theta}{6\mu_v} \delta^3 \right)}{\frac{h'_{fg} \rho_v}{R} \left(\frac{3U \sin\theta}{4} + \frac{9\rho_l U^2}{16\mu_v R} \sin\theta \cos\theta \delta^2 + \frac{\Delta\rho_l g \sin\theta}{4\mu_v} \delta^2 \right)} \quad (2.42)$$

The non-dimensional form of equation 2.42 is shown below (the steps to non-dimensionalize equation 2.42 is given in the appendix).

$$\frac{d\left(\frac{\delta}{D}\right)}{d\theta} = \frac{1}{1 + \frac{3\rho_l}{2\rho_v} Re_v \left(\frac{\delta}{D}\right)^2 \cos\theta + \frac{1}{3} \left(\frac{\delta}{D}\right)^2 \frac{Gr}{Re_v}} \left(\frac{2J_v}{3Pe_v \sin\theta \left(\frac{\delta}{D}\right)} + \frac{2q_r}{3\rho_v U h'_{fg} \sin\theta} - \right. \\ \left. 2 \left(\frac{\delta}{D}\right) \cot\theta - \frac{1}{2} \frac{\rho_l}{\rho_v} Re_v \left(\frac{\delta}{D}\right)^3 \left(\frac{3 \cos^2 \theta - 1}{\sin\theta} \right) - \frac{2}{9} \frac{Gr}{Re_v} \left(\frac{\delta}{D}\right)^3 \cot\theta - \right. \\ \left. \frac{2 \frac{\rho_l}{\rho_v} J_l \sin\theta}{3 \left(\frac{\pi Pe_l}{3} \left(\frac{2}{3} - \cos\theta + \frac{\cos^3 \theta}{3} \right) \right)^{\frac{1}{2}}} \right). \quad (2.43)$$

Here, $Re_v = \frac{\rho_v U D}{\mu_v}$ is the vapor Reynolds number, $Gr = g \left(\frac{\rho_l}{\rho_v} - 1 \right) \frac{D^3}{\nu_v^2}$ is the Grashof number (representing the ratio of buoyancy force to the viscous force acting on a fluid), $J_v = \frac{C_{p_v} (T_b - T_{sat})}{h'_{fg}}$ and $J_l = \frac{C_{p_l} (T_{sat} - T_w)}{h'_{fg}}$ are the vapor and liquid Jakob numbers respectively (representing the sensible heat absorbed or released during the liquid vapor phase change in comparison to the latent heat), $Pe_v = \frac{DU}{\alpha_v}$ and $Pe_l = \frac{DU}{\alpha_l}$ are the vapor and liquid Peclet

numbers respectively (representing the ratio of convection by thermal diffusion). We will solve equation 2.43 by Runge Kutta 4th order method, for the initial conditions obtained by imposing $\frac{d\delta}{d\theta}\Big|_{\theta=0} = 0$. The condition is justified owing to the fact that the vapor layer thickness is initially very small, and grows along the sphere surface due to the addition of vapor because of boiling. Therefore, at $\theta = 0$ this increase in vapor layer is negligible.

2.4.1. Initial condition

We will now use $\frac{d\delta}{d\theta}\Big|_{\theta=0} = 0$ or $\frac{d(\frac{\delta}{D})}{d\theta}\Big|_{\theta=0} = 0$ in equation 2.43 to get the initial conditions.

$$\left(\frac{1}{1 + \frac{3\rho_l}{2\rho_v} Re_v \left(\frac{\delta}{D}\right)^2 \cos\theta + \frac{1}{3} \left(\frac{\delta}{D}\right)^2 \frac{Gr}{Re_v}} \left(\frac{2J_v}{3Pe_v \sin\theta \left(\frac{\delta}{D}\right)} + \frac{2q_r}{3\rho_v U h'_{fg} \sin\theta} - 2 \left(\frac{\delta}{D}\right) \cot\theta - \frac{1}{2} \frac{\rho_l}{\rho_v} Re_v \left(\frac{\delta}{D}\right)^3 \left(\frac{3\cos^2\theta - 1}{\sin\theta} \right) - \frac{2}{9} \frac{Gr}{Re_v} \left(\frac{\delta}{D}\right)^3 \cot\theta - \frac{2\rho_l J_l \sin\theta}{3 \left(\frac{\pi Pe_l}{3} \left(\frac{2}{3} - \cos\theta + \frac{\cos^3\theta}{3} \right) \right)^{\frac{1}{2}}} \right) \right) \Big|_{\theta=0} = 0 \quad (2.44)$$

\Rightarrow

$$\left(\frac{2J_v}{3Pe_v \sin\theta \left(\frac{\delta}{D}\right)} + \frac{2q_r}{3\rho_v U h'_{fg} \sin\theta} - 2 \left(\frac{\delta}{D}\right) \cot\theta - \frac{1}{2} \frac{\rho_l}{\rho_v} Re_v \left(\frac{\delta}{D}\right)^3 \left(\frac{3\cos^2\theta - 1}{\sin\theta} \right) - \frac{2}{9} \frac{Gr}{Re_v} \left(\frac{\delta}{D}\right)^3 \cot\theta - \frac{2\rho_l J_l \sin\theta}{3 \left(\frac{\pi Pe_l}{3} \left(\frac{2}{3} - \cos\theta + \frac{\cos^3\theta}{3} \right) \right)^{\frac{1}{2}}} \right) \Big|_{\theta=0} = 0 \quad (2.45)$$

Multiplying above equation by $\frac{\delta}{D} \sin\theta$ we get

$$\left(\frac{2J_v}{3Pe_v} + \frac{2q_r \frac{\delta}{D}}{3\rho_v U h'_{fg}} - 2 \cos\theta \left(\frac{\delta}{D}\right)^2 - \frac{1}{2} \frac{\rho_l}{\rho_v} Re_v (3\cos^2\theta - 1) \left(\frac{\delta}{D}\right)^4 - \frac{2}{9} \frac{Gr}{Re_v} \cos\theta \left(\frac{\delta}{D}\right)^4 - \frac{2\rho_l J_l \sin^2\theta \frac{\delta}{D}}{3 \left(\frac{\pi Pe_l}{3} \left(\frac{2}{3} - \cos\theta + \frac{\cos^3\theta}{3} \right) \right)^{\frac{1}{2}}} \right) \Big|_{\theta=0} = 0 \quad (2.46)$$

\Rightarrow

$$\frac{2J_v}{3Pe_v} + \frac{2q_r \frac{\delta}{D}}{3\rho_v U h'_{fg}} - 2 \left(\frac{\delta}{D}\right)^2 - \frac{\rho_l}{\rho_v} Re_v \left(\frac{\delta}{D}\right)^4 - \frac{2}{9} \frac{Gr}{Re_v} \left(\frac{\delta}{D}\right)^4 - \frac{2\rho_l J_l \sin^2\theta \frac{\delta}{D}}{3 \left(\frac{\pi Pe_l}{3} \left(\frac{2}{3} - \cos\theta + \frac{\cos^3\theta}{3} \right) \right)^{\frac{1}{2}}} \Big|_{\theta=0} = 0 \quad (2.47)$$

The last term in equation 2.47 is solved separately as follows (the steps to solve last term in equation 2.47 is given in the appendix),

$$\lim_{\theta \rightarrow 0} \frac{2 \frac{\rho_l}{\rho_v} J_l \sin^2 \theta \frac{\delta}{D}}{3 \left(\frac{\pi P e_l}{3} \left(\frac{2}{3} - \cos \theta + \frac{\cos^3 \theta}{3} \right) \right)^{\frac{1}{2}}} \Bigg|_{\theta=0} = \frac{4}{\sqrt{3 \pi P e_l}} \frac{\rho_l}{\rho_v} J_l \frac{\delta}{D} \quad (2.48)$$

substituting equation 2.48 in equation 2.47 we get,

$$\frac{2J_v}{3Pe_v} + \frac{2q_r}{3\rho_v U h'_{fg}} \left(\frac{\delta}{D} \right) - 2 \left(\frac{\delta}{D} \right)^2 - \frac{\rho_l}{\rho_v} Re_v \left(\frac{\delta}{D} \right)^4 - \frac{2}{9} \frac{Gr}{Re_v} \left(\frac{\delta}{D} \right)^4 - \frac{4}{\sqrt{3 \pi P e_l}} \frac{\rho_l}{\rho_v} J_l \left(\frac{\delta}{D} \right) = 0 \quad (2.49)$$

\Rightarrow

$$\left(\frac{\rho_l}{\rho_v} Re_v + \frac{2}{9} \frac{Gr}{Re_v} \right) \left(\frac{\delta}{D} \right)^4 + 2 \left(\frac{\delta}{D} \right)^2 + \left(\frac{4}{\sqrt{3 \pi P e_l}} \frac{\rho_l}{\rho_v} J_l - \frac{2q_r}{3\rho_v U h'_{fg}} \right) \left(\frac{\delta}{D} \right) - \frac{2J_v}{3Pe_v} = 0 \quad (2.50)$$

Equation 2.50 is solved and the real, non-negative values of $\frac{\delta}{D}$ are the initial condition to solve equation 2.43. Equation 2.50 consists of various non-dimensional terms which are required to be evaluated from the properties of vapor and liquid evaluated at corresponding mean film temperature. The mean film temperature for vapor is $\frac{T_b + T_{sat}}{2}$ and for liquid is $\frac{T_{sat} + T_w}{2}$. Note that equation 2.43 has a singularity at $\theta = 0^\circ$ and 180° . Therefore the initial condition required to solve equation 2.43 by Runge-Kutta method is given at some θ near to 0° and not exactly at $\theta = 0^\circ$.

After calculating the variation of $\delta(\theta)$ we can compute the heat transfer coefficient, and the Nusselt number. We consider the fact that the energy leaving the sphere surface has two components namely conduction across the vapor film, and radiation (see figure 2). Therefore, an energy balance enables us to write:

$$h_\theta (T_b - T_{sat}) = \frac{k_v (T_b - T_{sat})}{\delta} + q_r, \quad (2.51)$$

$$h_\theta = \frac{k_v}{\delta} + \frac{q_r}{T_b - T_{sat}}, \quad (2.52)$$

where h_θ represents the local heat transfer coefficient. The local Nusselt number, Nu_θ is defined as $\frac{h_\theta D}{k_v}$, and therefore, can be written as,

$$Nu_\theta = \frac{D}{\delta} + \frac{D q_r}{k_v (T_b - T_{sat})}. \quad (2.53)$$

From the local Nusselt number, we can calculate the average Nusselt number using the total sphere area $4\pi R^2$ as follows:

$$Nu = \frac{1}{2} \int_0^{\theta_s} Nu_\theta \sin \theta d\theta, \quad (2.54)$$

here θ_s is the angle at which separation takes place. The reason for using θ_s in equation 2.54 indicates the validation of the analytical solutions till the point of separation. We further use 2.54, to calculate the averaged heat transfer coefficient:

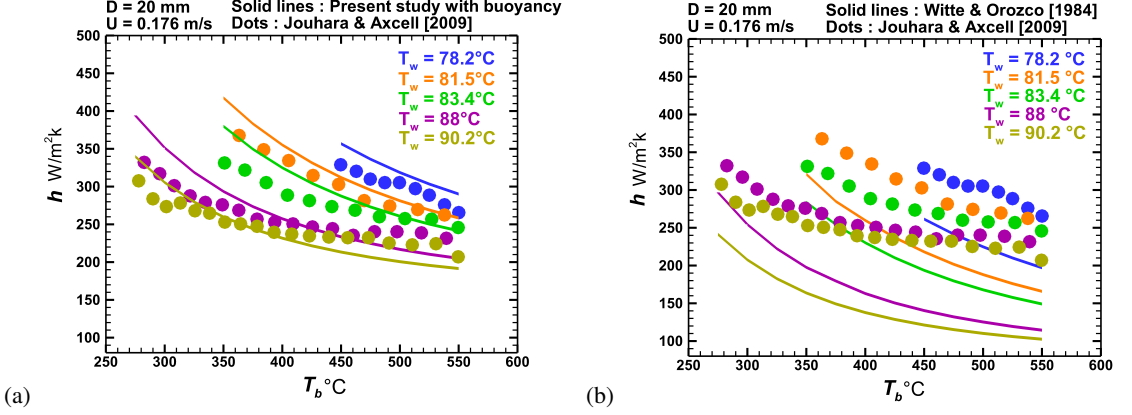


Figure 3: Comparison of the heat transfer coefficient with sphere temperature between (a) present study, and the experiment of Jouhara & P.Axcell (2009), (b) Witte & Orozco (1984) and experiment by Jouhara & P.Axcell (2009).

$$h = \frac{NuD}{k_v}. \quad (2.55)$$

2.4.2. Flow Separation

We can use equation 2.30, and apply $\left. \frac{\partial u}{\partial y} \right|_{y=0} = 0$ to determine the angle of separation. This boundary condition is used because the point at which the flow separates will have a velocity profile such that the gradient of velocity with respect to normal to surface becomes zero.

$$\cos \theta_s = - \left(\frac{\frac{3U}{2\delta_s^2} + \frac{\Delta\rho g}{2\mu_v}}{\frac{9\rho_l U^2}{8\mu_v R}} \right) = - \left(\frac{4\mu_v R}{3\rho_l U \delta_s^2} + \frac{4Rg\Delta\rho}{9U^2 \rho_l} \right), \quad (2.56)$$

where δ_s is the thickness of the vapor layer at the point of separation. The vapor layer grows as we move in direction of θ . As we reach a point where $\theta = \theta_s$, δ is equal to δ_s .

Equation 2.56 does not predict the separation angle directly, rather it needs to be solved simultaneously with equation 2.43. We can also observe from equation 2.56 that $\theta_s > \frac{\pi}{2}$. The second term in equation 2.56 represents the effect of buoyancy and scales with $\frac{1}{U^2}$. This signifies that at low velocities this term will grow rapidly and will suppress the separation resulting in an increase in the separation angle (see section 3).

3. Results

The comparison of the variation of heat transfer coefficient with sphere temperature between the present model, and the experiments of Jouhara & P.Axcell (2009) is shown in figure 3 (a). We also show the corresponding comparison between the model of Witte & Orozco (1984), and the experimental study of Jouhara & P.Axcell (2009) in figure 3 (b). Our model achieves a very good agreement with the results from the experiments. The model of Witte & Orozco (1984) manifests a significant departure from the experimental results. The reason being the inclusion of buoyancy in our model that successfully captures the delayed separation. We

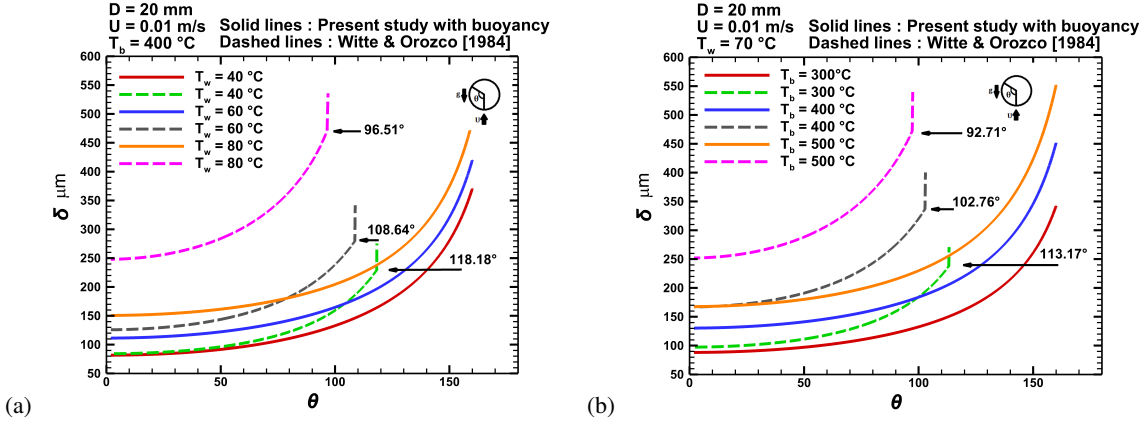


Figure 4: Variation of vapor boundary layer thickness over sphere at free stream velocity $U = 0.01\text{ m/s}$ with (a) bulk water temperature T_w at $T_b = 400^\circ\text{C}$, and (b) sphere temperature T_b at $T_w = 70^\circ\text{C}$.

further discuss the key role of buoyancy in delaying the separation at low velocities in the upcoming text.

The vapor boundary layer thickness δ increases with an increase in temperature of water (T_w), and an increase in sphere temperature (T_b) as can be observed from figures 4 (a) and (b) respectively. With an increase in the temperature of water T_w , the contribution of vapor film to the net energy exchange between the sphere, and the surrounding liquid decreases. Therefore, the energy going into the bulk liquid decreases, and the amount of total energy available for vaporization of liquid increases resulting in an increase in the vapor boundary layer thickness. Similarly, with an increase in sphere temperature T_b , the energy available for vaporization of the liquid increases resulting in an increase in vapor boundary layer thickness. At low velocities, the adverse pressure gradient weakens, and buoyancy (acting upwards) pushes the fluid against this weak adverse pressure gradient to delay the separation. Our model captures this separation delay for different T_w , and T_b as manifested in figures 4 (a) and (b). The model of Witte & Orozco (1984) owing to the exclusion of buoyancy predicts significantly early separation at low velocities as indicated by the rapid rise in the vapor boundary layer thickness in figures 4 (a) and (b).

We report a decrease in the vapor boundary layer thickness with an increase in free stream velocity U for a given value of the sphere and the water temperature in figure 5. It can be observed from figure 5 (a) that the separation is delayed (shown by the sudden increase in δ) with decreasing velocity. When the velocity becomes sufficiently low there is no separation which is similar to the observations of Bromley *et al.* (1953). In comparison to our model, the model of Witte & Orozco (1984) does not show any variation of separation angle with velocity (see figure 5 (b)). To understand the reason for the separation even at low velocities we analyze the expression of the angle of separation ($\cos\theta_s = -\left(\frac{4\mu_v R}{3\rho_l U \delta_s^2}\right)$) from the model of Witte & Orozco (1984). At a given T_w and T_b the product of U and δ_s^2 remains constant as shown in table 1. Therefore, the denominator in the expression of $\cos\theta_s$ will remain a constant and, therefore the separation angle will remain the same with velocity.

Our expression for θ_s is composed of two terms, $\frac{4\mu_v R}{3\rho_l U \delta_s^2}$ and $\frac{4Rg\Delta\rho}{9U^2\rho_l}$. The second term

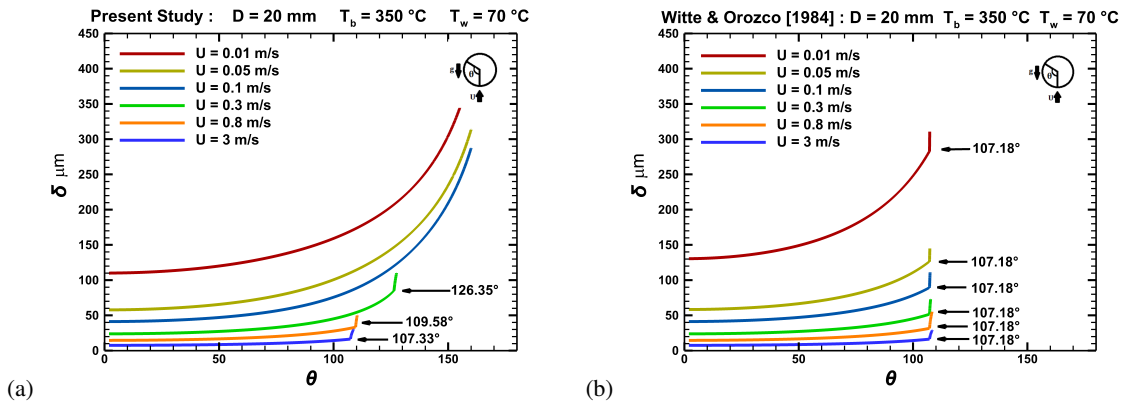


Figure 5: Variation of vapor boundary layer thickness over the sphere at different velocities for given sphere and bulk water temperature obtained from (a) present study, and (b) the model of Witte & Orozco (1984).

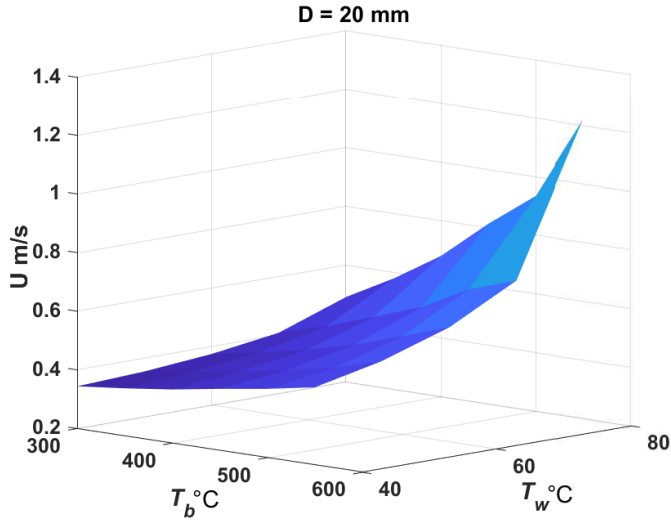
U (m/s)	δ_s (μm)	θ_s	$U * \delta_s^2 * 10^{12}$
3	16.34	107.18°	801.1
0.8	31.64	107.18°	801.1
0.3	51.68	107.18°	801.1
0.1	89.51	107.18°	801.1
0.05	126.58	107.1°	801.1
0.01	283.03	107.18°	801.1

Table 1: Model of Witte & Orozco (1984) at $T_w = 70^\circ\text{C}$, $T_b = 350^\circ\text{C}$, $D = 20$ mm

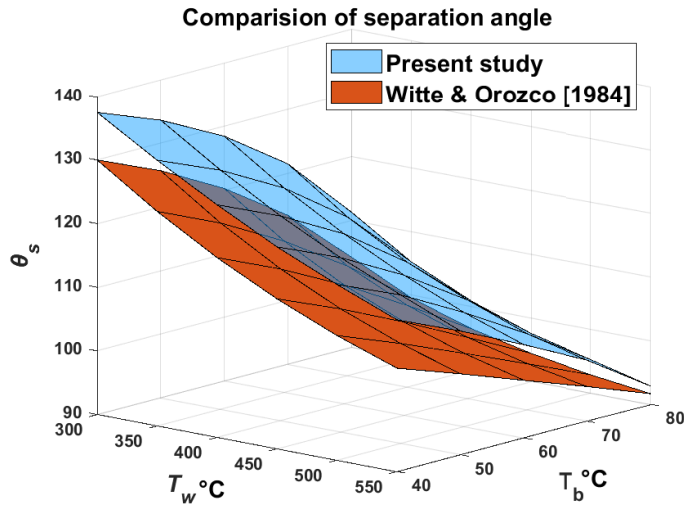
U (m/s)	δ_s (μm)	First term	Second term	First term + Second term	θ_s
3	16.41	0.2931	0.0048	0.2979	107.33°
0.8	33.28	0.2671	0.0681	0.3352	109.58°
0.5	45.91	0.2246	0.1744	0.3990	113.51°
0.3	85.26	0.1085	0.4844	0.5930	126.35°
0.1		No Separation			

Table 2: Present model at $T_w = 70^\circ\text{C}$, $T_b = 350^\circ\text{C}$, $D=20$ mm

represents the influence of buoyancy and scales with $\frac{1}{U^2}$. Therefore, decreasing the velocity, U , increases the second term. Table 2 demonstrates the variation of the first and second term with velocity for a given T_b and T_w . We can observe that as we decrease the velocity, the value of δ_s increases, the first term decreases, and the second increases. It can also be observed that the second term is negligible at high values of U , and doesn't contribute much in delaying the separation at high velocity. However, at low velocities,



(a) Surface plot of velocity, at which the first and the second terms in the expression for separation angle become equal, at different sphere and bulk water temperature obtained from the present study.



(b) Comparison of the surface plot of separation angle for the corresponding parameters of figure 6a obtained from present study and model of Witte & Orozco (1984).

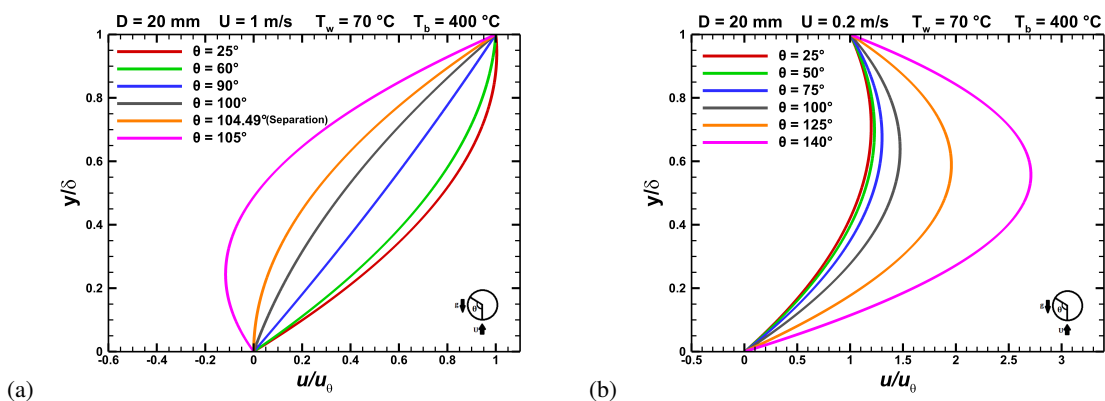
Figure 6

the contribution of buoyancy (second term) becomes significant resulting in separation delay.

We create a three-dimensional surface plot (see figure 6a) of the velocity, at which the first and the second terms in the expression for separation angle becomes equal, at different sphere, and water temperature. We present a data set comprising of the values of the first and the second terms in the expression for separation angle in table 3. Comparative three-dimensional surface plots (figure 6b) of the variation of the separation angle with respect

T_w °C	T_b °C	U (m/s)	δ_s (μm)	First term	Second term	First term + Second term	θ_s
40	300	0.344	41.72	0.3684	0.3684	0.7368	137.46°
70	350	0.455	49.72	0.2105	0.2105	0.4210	114.89°
80	400	0.68	62.65	0.0943	0.0943	0.1886	100.87°
80	450	0.82	70.46	0.0657	0.0657	0.1314	97.55°
80	550	1.22	95.01	0.0280	0.0280	0.0575	93.30°

Table 3: A representative dataset for figure 6a

Figure 7: Non-dimensional velocity profile (refer equation 2.3 for the expression of u_θ) at (a) $U = 1$ m/s, $T_w = 70^\circ\text{C}$, $T_b = 400^\circ\text{C}$, and (b) $U = 0.2$ m/s, $T_w = 70^\circ\text{C}$, $T_b = 400^\circ\text{C}$

to the sphere, and the water temperature are also generated by using the corresponding parameters of figure 6a for the present model, and the model of Witte & Orozco (1984). The region in figure 6b, where the surface generated by the present model is away from the surface generated by the model of Witte & Orozco (1984) corresponds to a region of low velocities in figure 6a. Similarly, the region in figure 6b, where the two surfaces are closer to each other, corresponds to a region of high velocities in figure 6a. Therefore, even when the first and the second terms in the expression of separation angle are equal the buoyancy may not be significant as can be seen at high velocities where the difference in the separation angle for the present model with the model of Witte & Orozco (1984) diminishes. Hence, we can conclude that at a particular sphere, and bulk water temperature, the influence of buoyancy is significant at lower velocities where the difference in the separation angle for present model and model of Witte & Orozco (1984) is significant. Clearly the model of Witte & Orozco (1984) under predicts the separation angle at all velocities owing to the exclusion of buoyancy in their analysis.

According to equation 2.29 the pressure gradient is favorable in the bottom half of the sphere ($\theta < 90^\circ$) whereas it is adverse in the top half ($\theta > 90^\circ$) of the sphere. Buoyancy favors the flow of the vapor in both the lower and the upper halves. When the velocity is high the adverse pressure gradient in the top half is also large, and even though buoyancy supports the vapor flow, the flow may separate. As the velocity decreases, the adverse pressure gradient

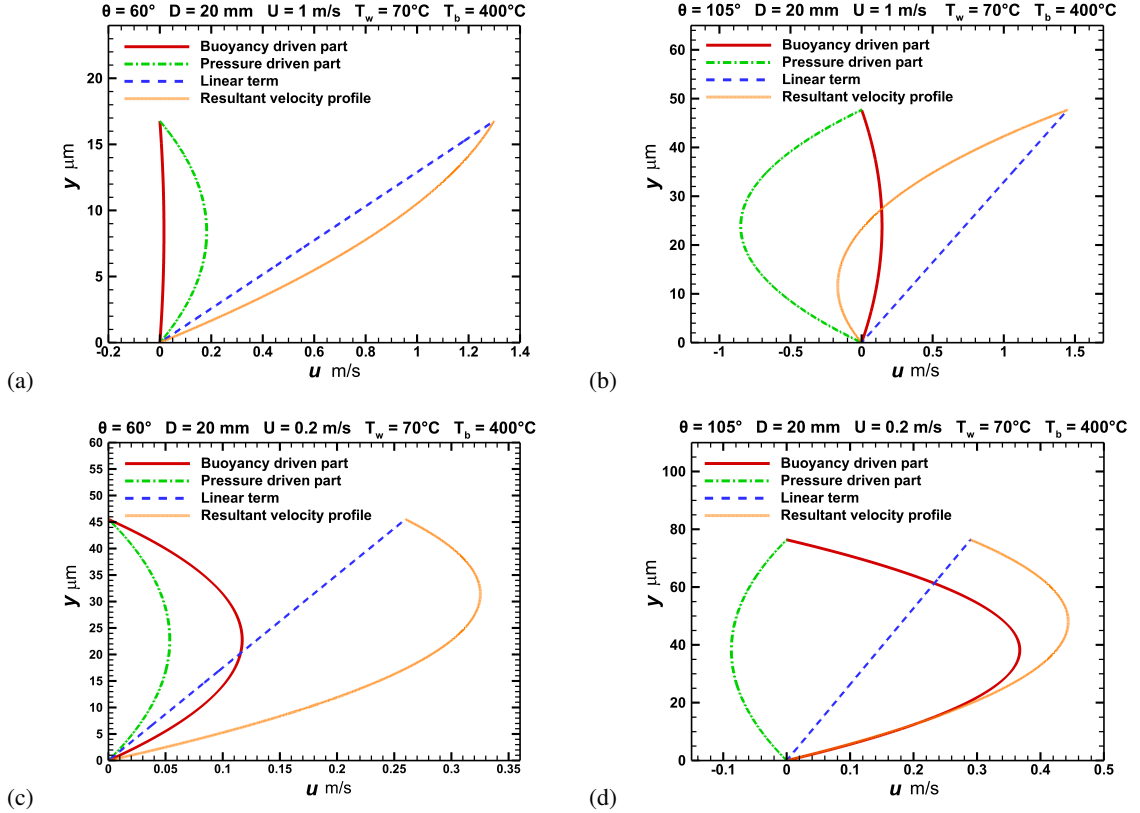


Figure 8: Dimensional velocity profile (refer equation 2.30) at different values of θ for $U = 1$ m/s and $U = 0.2$ m/s

in the top half of the sphere decreases, and buoyancy dominates the vapor flow resulting in delayed or no separation. Figures 7 (a) and (b) represent the non-dimensional velocity profiles at different angles for high, and low velocities respectively. At high velocity (figure 7 (a)) it can be observed that separation takes place in the top half of the sphere but at low velocity (figure 7(b)) we do not observe any separation. To further access the role of buoyancy in suppressing the separation we plot the three components in equation 2.30 in figures 8 for two different velocities at two different angles. We can observe that for $U = 1$ m/s and 0.2 m/s at $\theta = 60^\circ$, which represents a location at the bottom half of the sphere, both the pressure and the buoyancy are assisting the flow of vapor (see figures 8 (a) and (c)). However, at $\theta = 105^\circ$, which represents a location at the upper half of the sphere, the pressure gradient is adverse and it competes with buoyancy to get the flow separated for $U = 1$ m/s and delay the separation for $U = 0.2$ m/s (figures 8 (b) and (d) respectively).

4. Conclusion

A theoretical investigation is performed to understand the influence of buoyancy on the heat transfer characteristics and boundary layer separation behavior due to film boiling from a slowly moving heated sphere. The novelty of this study lies in the inclusion of the buoyancy in the governing equation unprecedented to the previous theoretical investigations for a

spherical body. In the present analytical model the momentum, and the energy equations are solved in the vapor phase to obtain the velocity, and the temperature distribution in terms of the vapor layer thickness. We apply an energy balance at the vapor-liquid interface to determine the vapor layer thickness. The flow of liquid around the sphere is considered to be governed by potential theory, and the energy equation in liquid is then solved for the known velocity distribution.

We find that the film boiling heat transfer coefficient decreases with an increase in sphere, and bulk water temperature owing to a subsequent increase in the vapor layer thickness. This behavior of the heat transfer coefficient resembles closely to the experimental results reported by Jouhara & P.Axcell (2009). We also found that buoyancy plays a very significant role at low velocities in delaying the separation and allows the heat transfer calculation from a larger area. We have included buoyancy in the expression of the vapor velocity that resulted in capturing the delayed separation phenomenon similar to the observations of by Bromley *et al.* (1953) and Kobayasi & Kiyosi (1965). We further analyzed the dependence of the flow separation behavior on the relative magnitudes of the pressure gradient, and buoyancy. At high velocity the pressure gradient overshadows the buoyancy effects, and the flow separates. However, at sufficiently low velocities buoyancy drives the flow against the adverse pressure gradient, and separation is not observed. Therefore, it can be concluded that the inclusion of buoyancy is imperative for capturing the correct variation of the heat transfer characteristics, and the boundary layer separation phenomenon at low velocities.

REFERENCES

- BRADFIELD, W. S. 1966 Liquid-solid contact in stable film boiling. *Ind. and Eng. Chemn Fundamentals* **5**, 201–204.
- BRADFIELD, W. S. 1967 On the Effect of Subcooling on Wall Superheat in Pool Boiling. *Journal of Heat Transfer* **89** (3), 269–270.
- BROMLEY, LEROY A, LEROY, NORMAN R & ROBBERS, JAMES A 1953 Heat transfer in forced convection film boiling. *Industrial & Engineering Chemistry* **45** (12), 2639–2646.
- BURNS, R. A. 1989 Heat transfer studies with application to nuclear reactors. PhD thesis, Thesis, University of Manchester.
- DHIR, V.K. & PUROHIT, G.P. 1978 Subcooled film-boiling heat transfer from spheres. *Nuclear Engineering and Design* **47** (1), 49–66.
- HESSON, JC & WITTE, LC 1966 Comment on “film boiling heat transfer around a sphere in forced convection” by k. kobayasi. *Journal of Nuclear Science and Technology* **3** (10), 448–449.
- JOUHARA, H. & P.AXCELL, B. 2009 Film boiling heat transfer and vapour film collapse on spheres, cylinders and plane surfaces. *Nuclear Engineering and Design*. **239**, 1885–1900.
- KOBAYASI & KIYOSI 1965 Film boiling heat transfer around a sphere in forced convection. *Journal of Nuclear Science and Technology* **2** (2), 62–67.
- KUTATELADZE, S. S. 1959 Liquid-Metal Heat Transfer Media. In *In Interactive dynamics of convection and solidification*, pp. 77–81. Springer US.
- MOTTE, EUGENE I & BROMLEY, LEROY A 1957 Film boiling of flowing subcooled liquids. *Industrial & Engineering Chemistry* **49** (11), 1921–1928.
- SIDEMAN, S. 1966 The equivalence of the penetration theory and potential flow theories. *Ind. and Eng. Chemn Fundamentals* **58**, 54–58.
- VAKARELSKI, IVAN U, MARSTON, JEREMY O, CHAN, DEREK YC & THORODDSEN, SIGURDUR T 2011 Drag reduction by leidenfrost vapor layers. *Physical review letters* **106** (21), 214501.
- WALFORD, FJ 1969 Transient heat transfer from a hot nickel sphere moving through water. *International Journal of Heat and Mass Transfer* **12** (12), 1621–1625.
- WITTE, L. C. 1967 heat transfer from a sphere to liquid sodium during forced convection. PhD thesis, Oklahoma State University, <https://digital.library.unt.edu/ark:/67531/metadc1024053/>.

- WITTE, L. C. 1968a An Experimental Study of Forced-Convection Heat Transfer From a Sphere to Liquid Sodium. *Journal of Heat Transfer* **90** (1), 9–12.
- WITTE, L. C. 1968b Film boiling from a sphere. *Industrial & Engineering Chemistry Fundamentals* **7** (3), 517–518.
- WITTE, L. C. & OROZCO, J. 1984 The Effect of Vapor Velocity Profile Shape on Flow Film Boiling From Submerged Bodies. *Journal of Heat Transfer* **106** (1), 191–197.

Appendix

Steps to non-dimensionalize equation 2.42 :

Consider equation 2.42,

$$\frac{d\delta}{d\theta} = \frac{1}{\frac{h'_{fg}\rho_v}{R} \left(\frac{3U \sin \theta}{4} + \frac{9\rho_l U^2}{16\mu_v R} \sin \theta \cos \theta \delta^2 + \frac{\Delta\rho g \sin \theta}{4\mu_v} \delta^2 \right)} \left(\frac{k_v (T_b - T_{sat})}{\delta} + \sigma \epsilon (T_b^4 - T_{sat}^4) - \frac{k_l \Delta T_w \sin^2 \theta}{\sqrt{\pi M \eta}} - \frac{h'_{fg}\rho_v}{R} \left(\frac{3U \cos \theta \delta}{2} + \frac{3\rho_l U^2}{16\mu_v R} (3 \cos^2 \theta - 1) \delta^3 + \frac{\Delta\rho g \cos \theta}{6\mu_v} \delta^3 \right) \right) \quad (1)$$

To non-dimensionalize the above equation we first divide the numerator and denominator by $\frac{h'_{fg}\rho_v}{R} \frac{3U \sin \theta}{4}$. We first consider the non-dimensionalization of denominator as follows:

$$\frac{h'_{fg}\rho_v}{R} \left(\frac{3U \sin \theta}{4} + \frac{9\rho_l U^2}{16\mu_v R} \sin \theta \cos \theta \delta^2 + \frac{\Delta\rho g \sin \theta}{4\mu_v} \delta^2 \right), \quad (2)$$

⇒

$$\frac{h'_{fg}\rho_v}{R} \frac{3U \sin \theta}{4} \left(1 + \frac{3\rho_l U \cos \theta \delta^2}{4\mu_v R} + \frac{\Delta\rho g \delta^2}{3\mu_v U} \right), \quad (3)$$

⇒

$$\frac{h'_{fg}\rho_v}{R} \frac{3U \sin \theta}{4} \left(1 + \frac{3}{2} \frac{\rho_l}{\rho_v} \frac{\rho_v U D}{\mu_v} \left(\frac{\delta}{D} \right)^2 \cos \theta + \frac{\Delta\rho g}{3U} \frac{\delta^2}{\mu_v} \right), \quad (4)$$

⇒

$$\frac{h'_{fg}\rho_v}{R} \frac{3U \sin \theta}{4} \left(1 + \frac{3}{2} \frac{\rho_l}{\rho_v} Re_v \left(\frac{\delta}{D} \right)^2 \cos \theta + \frac{\Delta\rho g}{3U} \frac{\delta^2}{\mu_v} \right), \quad (5)$$

⇒

$$\frac{h'_{fg}\rho_v}{R} \frac{3U \sin \theta}{4} \left(1 + \frac{3}{2} \frac{\rho_l}{\rho_v} Re_v \left(\frac{\delta}{D} \right)^2 \cos \theta + \frac{Gr}{3Re_v} \left(\frac{\delta}{D} \right)^2 \right). \quad (6)$$

Now, dividing the numerator and denominator by $\frac{h'_{fg}\rho_v}{R} \frac{3U \sin \theta}{4}$, we can rewrite the denominator as

$$1 + \frac{3}{2} \frac{\rho_l}{\rho_v} Re_v \left(\frac{\delta}{D} \right)^2 \cos \theta + \frac{Gr}{3Re_v} \left(\frac{\delta}{D} \right)^2. \quad (7)$$

Now, consider the numerator of equation 2.42,

$$\frac{1}{\frac{h'_{fg}\rho_v}{R} \frac{3U \sin \theta}{4}} \frac{1}{D} \left(\frac{k_v (T_b - T_{sat})}{\delta} + \sigma \epsilon (T_b^4 - T_{sat}^4) - \frac{k_l \Delta T_w \sin^2 \theta}{\sqrt{\pi M \eta}} - \frac{h'_{fg}\rho_v}{R} \left(\frac{3U \cos \theta \delta}{2} + \frac{3\rho_l U^2}{16\mu_v R} (3 \cos^2 \theta - 1) \delta^3 + \frac{\Delta \rho g \cos \theta}{6\mu_v} \delta^3 \right) \right). \quad (8)$$

Term $\frac{1}{D}$ in the above expression comes from the non-dimensionalization of the left hand side of equation 2.42 and $\frac{d\delta}{d\theta}$ is written as $\frac{d(\delta/D)}{d\theta} D$. We now non-dimensionalize all the terms of the above equation, Consider the first term,

(i)

$$\begin{aligned} & \frac{1}{D} \frac{k_v (T_b - T_{sat})}{\frac{h'_{fg}\rho_v}{R} \frac{3U \sin \theta}{4}} \\ \Rightarrow & \\ & \frac{2Cp_v (T_b - T_{sat})}{3h_{fg}} \frac{k_v}{Cp_v \rho_v U \sin \theta \delta}, \\ \Rightarrow & \\ & \frac{2J_v}{3 \frac{\rho_v Cp_v}{k_v} U D \frac{\delta}{D} \sin \theta} \\ \Rightarrow & \\ & \frac{2J_v}{3Pe_v \frac{\delta}{D} \sin \theta}. \end{aligned} \quad (9)$$

Consider the second term,

(ii)

$$\begin{aligned} & \frac{1}{D} \frac{q_r}{\frac{h'_{fg}\rho_v}{R} \frac{3U \sin \theta}{4}}, \\ \Rightarrow & \\ & \frac{2q_r}{3\rho_v U h_{fg} \sin \theta}. \end{aligned} \quad (10)$$

Consider the third term,

(iii)

$$\frac{1}{D} \frac{\frac{k_l \Delta T_w \sin^2 \theta}{\sqrt{\pi M \eta}}}{\frac{h'_{fg}\rho_v}{R} \frac{3U \sin \theta}{4}},$$

\Rightarrow

$$\begin{aligned} & \frac{2Cp_l(T_{sat} - T_w)}{3h'_{fg}} \frac{k_l}{Cp_l\rho_v} \frac{\sin\theta}{\sqrt{\pi M\eta}} \frac{1}{U}, \\ \Rightarrow & \\ & \frac{2}{3} J_l \alpha_l \frac{\rho_l}{\rho_v} \frac{\sin\theta}{\sqrt{\pi M\eta}} \frac{1}{U}. \end{aligned}$$

Substituting the values of M and η we get,

\Rightarrow

$$\frac{2}{3} J_l \frac{\rho_l}{\rho_v} \sin\theta \frac{1}{\sqrt{\left(\frac{\pi Pe_l}{3} \left(\frac{2}{3} - \cos\theta + \frac{\cos^3\theta}{3}\right)\right)}}. \quad (11)$$

Consider the fourth term,

(iv)

$$\frac{1}{D} \frac{\frac{h'_{fg}\rho_v}{R} \frac{3U \cos\theta}{2} \delta}{\frac{h'_{fg}\rho_v}{R} \frac{3U \sin\theta}{4}},$$

\Rightarrow

$$2 \cot\theta \left(\frac{\delta}{D}\right). \quad (12)$$

Consider the fifth term,

(v)

$$\frac{1}{D} \frac{\frac{h'_{fg}\rho_v}{R} \frac{3\rho_l U^2}{16\mu_v R} (3\cos^2\theta - 1)\delta^3}{\frac{h'_{fg}\rho_v}{R} \frac{3U \sin\theta}{4}},$$

\Rightarrow

$$\frac{1}{2} \left(\frac{\delta}{D}\right)^3 \frac{D}{\mu_v} \rho_l U \left(\frac{3\cos^2\theta - 1}{\sin\theta}\right),$$

\Rightarrow

$$\frac{1}{2} \left(\frac{\delta}{D}\right)^3 \frac{\rho_l}{\rho_v} \frac{\rho_v U D}{\mu_v} \left(\frac{3\cos^2\theta - 1}{\sin\theta}\right),$$

\Rightarrow

$$\frac{1}{2} \left(\frac{\delta}{D}\right)^3 \frac{\rho_l}{\rho_v} Re_v \left(\frac{3\cos^2\theta - 1}{\sin\theta}\right). \quad (13)$$

Consider the sixth term,

(vi)

$$\frac{1}{D} \frac{\frac{\Delta\rho g \cos\theta}{6\mu_v} \delta^3}{\frac{h'_{fg}\rho_v}{R} \frac{3U \sin\theta}{4}},$$

\Rightarrow

$$\frac{2}{9} \left(\frac{\delta}{D} \right)^3 D^2 \cot \theta \frac{\Delta \rho g}{U \mu_v},$$

⇒

$$\frac{2}{9} \left(\frac{\delta}{D} \right)^3 \frac{Gr}{Re_v} \cot \theta. \quad (14)$$

Arranging all the terms, we finally get,

$$\begin{aligned} \frac{d\left(\frac{\delta}{D}\right)}{d\theta} = & \frac{1}{1 + \frac{3\rho_l}{2\rho_v} Re_v \left(\frac{\delta}{D}\right)^2 \cos \theta + \frac{1}{3} \left(\frac{\delta}{D}\right)^2 \frac{Gr}{Re_v}} \left(\frac{2J_v}{3Pe_v \sin \theta \left(\frac{\delta}{D}\right)} + \frac{2q_r}{3\rho_v U h'_{fg} \sin \theta} - \right. \\ & \left. 2 \left(\frac{\delta}{D}\right) \cot \theta - \frac{1}{2} \frac{\rho_l}{\rho_v} Re_v \left(\frac{\delta}{D}\right)^3 \left(\frac{3 \cos^2 \theta - 1}{\sin \theta} \right) - \frac{2}{9} \frac{Gr}{Re_v} \left(\frac{\delta}{D}\right)^3 \cot \theta - \right. \\ & \left. \frac{2 \frac{\rho_l}{\rho_v} J_l \sin \theta}{3 \left(\frac{\pi Pe_l}{3} \left(\frac{2}{3} - \cos \theta + \frac{\cos^3 \theta}{3} \right) \right)^{\frac{1}{2}}} \right). \quad (15) \end{aligned}$$

Steps to solve expression 2.48:

The last term in equation 2.47 has to be solved separately as follow,

$$\lim_{\theta \rightarrow 0} \frac{2 \frac{\rho_l}{\rho_v} J_l \sin^2 \theta \frac{\delta}{D}}{3 \left(\frac{\pi Pe_l}{3} \left(\frac{2}{3} - \cos \theta + \frac{\cos^3 \theta}{3} \right) \right)^{\frac{1}{2}}} \quad (16)$$

The above equation can be written as

$$\lim_{\theta \rightarrow 0} \frac{2 \frac{\rho_l}{\rho_v} J_l \sin^2 \theta \frac{\delta}{D}}{3 \left(\frac{\pi Pe_l}{9} (2 - 3 \cos \theta + \cos^3 \theta) \right)^{\frac{1}{2}}} \quad (17)$$

⇒

$$\frac{2 \frac{\rho_l}{\rho_v} \frac{J_l}{\sqrt{\pi Pe_l}} \frac{\delta}{D}}{3} \lim_{\theta \rightarrow 0} \frac{\sin^2 \theta}{(2 - 3 \cos \theta + \cos^3 \theta)^{\frac{1}{2}}} \quad (18)$$

Now, consider the denominator inside the limit in equation 18. It can be written as,

$$(1 - \cos \theta) (1 - \cos \theta) (2 + \cos \theta)$$

⇒

$$4 \sin^4 \frac{\theta}{2} (2 + \cos \theta)$$

The numerator inside the limit in equation 18 can be written as,

$$\sin^2 \theta = 4 \sin^2 \frac{\theta}{2} \cos^2 \frac{\theta}{2}$$

Therefore, equation 18 can be written as,

$$2 \frac{\rho_l}{\rho_v} \frac{J_l}{\sqrt{\pi P e_l}} \frac{\delta}{D} \lim_{\theta \rightarrow 0} \frac{4 \sin^2 \frac{\theta}{2} \cos^2 \frac{\theta}{2}}{\left(4 \sin^4 \frac{\theta}{2} (2 + \cos \theta)\right)^{\frac{1}{2}}} \quad (19)$$

\Rightarrow

$$2 \frac{\rho_l}{\rho_v} \frac{J_l}{\sqrt{\pi P e_l}} \frac{\delta}{D} \lim_{\theta \rightarrow 0} \frac{4 \sin^2 \frac{\theta}{2} \cos^2 \frac{\theta}{2}}{2 \sin^2 \frac{\theta}{2} (2 + \cos \theta)^{\frac{1}{2}}} \quad (20)$$

$$2 \frac{\rho_l}{\rho_v} \frac{J_l}{\sqrt{\pi P e_l}} \frac{\delta}{D} \lim_{\theta \rightarrow 0} \frac{2 \cos^2 \frac{\theta}{2}}{(2 + \cos \theta)^{\frac{1}{2}}} \quad (21)$$

Substituting the limit we get,

$$\frac{4}{\sqrt{3\pi P e_l}} \frac{\rho_l}{\rho_v} J_l \frac{\delta}{D} \quad (22)$$

Therefore, we can finally write,

$$\lim_{\theta \rightarrow 0} \frac{2 \frac{\rho_l}{\rho_v} J_l \sin^2 \theta \frac{\delta}{D}}{3 \left(\frac{\pi P e_l}{3} \left(\frac{2}{3} - \cos \theta + \frac{\cos^3 \theta}{3} \right) \right)^{\frac{1}{2}}} \Bigg|_{\theta} = - \frac{4}{\sqrt{3\pi P e_l}} \frac{\rho_l}{\rho_v} J_l \frac{\delta}{D} \quad (23)$$